Reliable optical characterization of e-beam evaporated TiO_2 films deposited at different substrate temperatures

T. Amotchkina,[1,2,*] M. Trubetskov,[1,2] A. Tikhonravov,[2] I. B. Angelov,[1] and V. Pervak[3,4]

[1]Max-Planck Institute of Quantum Optics, Hans-Kopfermann-Str. 1, 85748 Garching, Germany

[2]Research Computing Center, Moscow State University, Leninskie Gory, 119991 Moscow, Russia

[3]Ludwig-Maximilians-Universität München, Am Coulombwall 1, 85748 Garching, Germany

[4]Ultrafast Innovations GmbH Am Coulombwall 1, 85748 Garching, Germany

*Corresponding author: Tatiana@srcc.msu.ru

Received 9 August 2013; revised 23 September 2013; accepted 24 September 2013;
posted 24 September 2013 (Doc. ID 195504); published 11 October 2013

We studied e-beam evaporated TiO_2 films deposited at two different substrate temperatures between 120°C and 300°C. We reliably characterized the film samples on the basis of *in situ* and *ex situ* measurements. We carried out annealing on the samples and studied the induced changes in the properties of the films. The results can be useful for further laser-induced damage threshold investigations. © 2013 Optical Society of America

OCIS codes: (310.6860) Thin films, optical properties; (310.7005) Transparent conductive coatings.
http://dx.doi.org/10.1364/AO.53.0000A8

1. Introduction

In recent years, titanium dioxide (TiO_2) has been extensively studied because it is widely used as a high-index material in multilayer structures operating in visible and near infrared spectral ranges [1,2]. TiO_2 is used in combination with SiO_2 in optical coating production due to the high contrast of their refractive indices. TiO_2 exhibits interesting optical and electronic properties, chemical stability, good adhesion, and transparency in the visible and near infrared regions [3]. It is not surprising therefore, that many authors carry out research and publish results related to various aspects of TiO_2 amorphous films and crystalline structures. TiO_2 thin films can be produced by different deposition techniques including magnetron sputtering [4,5], RF sputtering [6,7], e-beam evaporation [8], reactive evaporation [3,9], plasma ion-assisted deposition [10], e-beam evaporation with ion-beam assistance [11,12], plasmatron sputtering [13], electrophoretic deposition [14], and solgel methods [15]. Some authors compare the properties of TiO_2 films produced by different methods (see, for example, [16,17]). In many papers optical characterization of TiO_2 samples is performed [3,4,7,10,11,13,15,16,18]. Structural and morphological characterization is carried out by using various experimental techniques [5,7,10,11,13,14,16,17,19]. Influence of different deposition parameters on the optical, electrical, and structural properties can be found in [5,6,9,11–13,17]. Electronic properties of TiO_2, including bandgap estimations, are obtained in the publications of several authors [7,8,12,14,15,20]. The optical and electronic properties of crystalline and amorphous TiO_2 structures calculated using quantum mechanical algorithms are reported in [19–21]. The effects of annealing on the optical, structural and electronic properties of TiO_2 films are considered by different researchers (see, for example, [6–8,10–12,17]).

1559-128X/14/0400A8-08$15.00/0
© 2014 Optical Society of America

The motivation for our research is based on the attractiveness of TiO_2 as high-index layer material in multilayer optical coatings for laser applications. The usage of TiO_2 in multilayers for lasers is restricted by its relatively low bandgap. It is known [22] that the bandgap values are decreasing with growing refractive index values, and for ultrashort pulses the laser-induced damage threshold (LIDT) of dielectrics is directly dependent on the bandgap of the high-index material [23–25] for sub-10-ps pulses [26]. TiO_2 films of relatively low packing density are supposed to have higher effective bandgaps than dense films and due to this they could be considered as high-index layers in coatings for laser applications. Therefore, an accurate study of the optical properties of e-beam evaporated TiO_2 films deposited under different deposition conditions would be useful for the potential applications of these films. In the present work we carefully characterized and compared the optical properties of e-beam evaporated TiO_2 films deposited at two different substrate temperatures. Also, we performed annealing of the TiO_2 samples and studied their effect on the optical constants and bandgap values of the TiO_2 films.

In Section 2 we describe experimental samples and measurement data. In Section 3 we provide a reliable optical characterization of the samples, which includes verification and validation of obtained results. In Section 4 we compare the optical constants and the bandgaps of the considered films before and after annealing. The final conclusions are presented in Section 5.

2. Experimental Samples and Measurement Data

For this study, four samples of single TiO_2 layers were prepared: two samples, named S1 and S3, on Glass B260 substrate of 1 mm thickness and two samples, named S2 and S4, on Suprasil substrate of 6.35 mm thickness. All four samples were produced by e-beam evaporation using SYRUSPro 710 deposition plant (Leybold Optics, Alzenau, Germany). Samples S1 and S2 were deposited at a relatively low substrate temperature of 120°. Samples S3 and S4 were prepared at a higher substrate temperature of 300°. The system was pumped down to 10^{-6} mbar before deposition. Oxygen was fed near the Ti_3O_5 targets to oxidize the evaporated material. The deposition rate was approximately 0.3 nm/s.

The SYRUSPro 710 deposition plant was equipped with broadband monitoring system (BBM) [27]. Samples S1 and S3 were placed on the calotte positions, where BBM measurements were performed. At the end of the depositions *in situ* transmittance data were recorded by the BBM device within a range from 400 to 950 nm with an approximately 0.5 nm wavelength step. The accuracy of *in situ* measurements ΔT can be estimated as 1.0%.

Two weeks after the deposition, the transmittances and reflectances of all samples were measured *ex situ* using a Perkin Elmer 950 spectrophotometer. The measurement accuracy ΔT is estimated as 0.2%. Measurements were performed in the spectral range from 320 to 1500 nm with a 1 nm wavelength step. Then, samples S2 and S4 were annealed at 300°C during 5 h. On the next day, the transmittance and reflectance spectra were measured again using a Perkin Elmer 950 spectrophotometer.

3. Characterization Results

In Fig. 1 we compare *in situ* and *ex situ* data related to samples S1 and S3. As evident from Fig. 1, the *ex situ* transmittance curves are shifted to the longer wavelengths with respect to those that are *in situ*. The shifts are more noticeable in the case of S1 sample deposited at low substrate temperature. These shifts can be explained by the structural difference between TiO_2 films in vacuum and in atmosphere. It is known that e-beam evaporated films have relatively low packing density [1]. After transferring these films from vacuum to atmosphere, their pores get filled with water. According to the Maxwell–Garnett formalism, this leads to an increase of the refractive index. As a consequence, the optical thickness of the film increases and the spectral curves shift to the longer wavelengths (a so-called vacuum shift) [1]. In the case of the S1 sample, this vacuum shift is larger than in the case of the S3 sample (Fig. 1).

We assume that the refractive indices and the extinction coefficients of the deposited films in the visible spectral range can be described by Cauchy and an exponential model, respectively [18]:

$$n(\lambda) = A_0 + \frac{A_1}{\lambda^2} + \frac{A_2}{\lambda^4},$$
$$k(\lambda) = B_0 \exp[B_2\lambda^{-1} + B_3\lambda]. \quad (1)$$

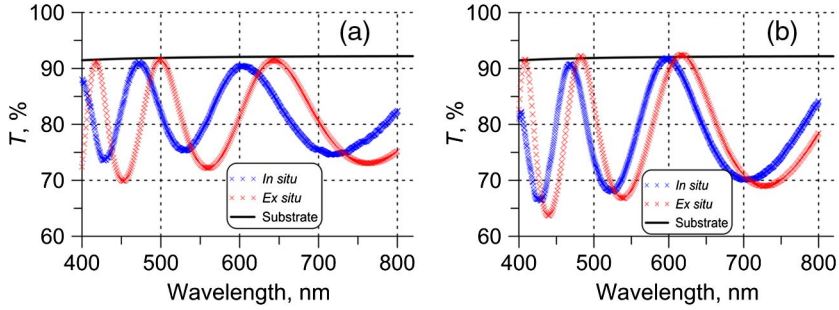

Fig. 1. Comparison of *in situ* and *ex situ* transmittance data related to samples S1 (a) and S2 (b).

The model parameters and film thickness d were found by minimization of a discrepancy function estimating closeness of experimental data to model spectral characteristics [18]. In the cases when only transmittance measurement data are available, only refractive index wavelength dependences and film thicknesses were determined [28]. The refractive index wavelength dependences of S1 and S3 TiO_2 films found from *in situ* and *ex situ* transmittance data are compared in Fig. 2. As expected, the refractive indices of the TiO_2 films in vacuum are lower than their refractive indices in atmosphere. The estimated values for physical thickness are quite close (see Table 1).

The offset Δn in a film refractive index caused by systematic errors in measurement transmittance data can be estimated as [29]

$$\Delta n = \frac{(n^2 + n_s)^3}{8nn_s(n_s - n^2)}\Delta T. \tag{2}$$

We use estimations of measurement accuracy presented in the end of Section 2. Substituting $n = 2.21$ and $n = 2.37$, $n_s = 1.46$, and $\Delta T = 0.2\%$ in Eq. (2), we obtain that the accuracy of refractive index determination from *ex situ* data is about 0.6%. Substituting $n = 2.1$ and $n = 2.28$, $n_s = 1.51$, and $\Delta T = 1.0\%$ into Eq. (2), we get accuracy of refractive index determination from *in situ* data that is about 3%.

To verify the obtained results, another characterization approach is applied. In the frame of this approach, the considered films are represented as a mixture of bulk material and voids. For any given wavelength, the film refractive index n can be described using Bruggemann's formula [30]:

$$n = \frac{1}{2}\sqrt{(3p-1)n_b^2 + (2-3p)n_v^2 + \sqrt{((3p-1)n_b^2 + (2-3p)n_v^2)^2 + 8n_b^2n_v^2}}, \tag{3}$$

where n_b and n_v are the refractive indices of the bulk material and voids, respectively; p is the volume fraction of the bulk material (packing density). In our characterization process, we considered the refractive index of dense ion-beam sputtered (IBS) TiO_2 films [18] as bulk refractive index (see Fig. 2). In the case of *in situ* and *ex situ* data, voids are assumed to be filled with vacuum and water, respectively. In the course of the characterization process, only two unknown parameters, p and d, were searched for. The refractive indices determined from the *in situ* and the *ex situ* measurements related to samples S1 and S3 are depicted in Fig. 2 by dashed curves. The obtained values of p and d are presented in Table 1. It is evident from Fig. 2 and Table 1 that the parameters obtained by the two different models are in a good agreement, which is an indication of the reliability of our characterization results.

It is interesting that the packing densities found for films in vacuum and in atmosphere are quite close. This may be an indirect confirmation of the supposition that water fills the pores after exposing the samples to atmosphere. The film thicknesses in the case of S1 and S3 samples increased in atmosphere in comparison with vacuum by 0.9% and 0.8%, respectively. This may indicate "swelling" of the films under atmospheric conditions. In the last column of Table 1 the approximate values of film densities ρ are presented. These values were obtained by Lorentz–Lorenz formalism [3]:

$$\frac{n^2 - 1}{n^2 + 2} = C\rho, \tag{4}$$

where $C = 0.1623$ cm^3/g. In Fig. 3 we show the theoretical dependence $n(\rho)$ found from Eq. (4) and the positions of experimental values $n(\rho)$ on this curve.

Characterization of the S2 and S4 samples is performed on the basis of transmittance and reflectance *ex situ* data using both approaches described above. Due to the fact that both reflectance and transmittance data are available, not only the refractive

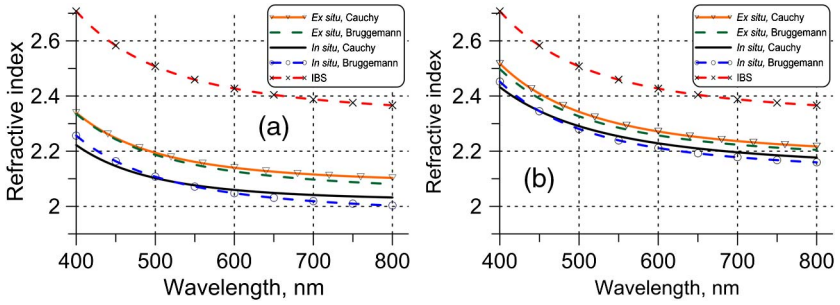

Fig. 2. Refractive indices of S1 (a) and S3 (b) films found from *ex situ* and *in situ* data using different models.

Table 1. Parameters of TiO_2 Films

Sample	Content	Model	Volume Fraction p, %	Thickness d, nm	n at 500 nm	Density ρ, g/cm^3
S1	TiO_2/Vacuum	Cauchy		453.9	2.06	3.2
		Bruggemann	74.1	444.7	2.1	
	TiO_2/Water	Cauchy		457.9	2.18	3.43
		Bruggemann	73.5	456.5	2.19	
S2	TiO_2/Water	Cauchy		457.3	2.21	3.48
		Bruggemann	74.9	458.7	2.20	
S3	TiO_2/Vacuum	Cauchy		405.2	2.28	3.6
		Bruggemann	85.0	404.5	2.28	
	TiO_2/Water	Cauchy		408.5	2.34	3.7
		Bruggemann	85.0	411.3	2.33	
S4	TiO_2/Water	Cauchy		398.6	2.37	3.7
		Bruggemann	88.1	400.2	2.37	

index, but also the extinction coefficient has been reliably determined. The main parameters of the samples are collected in Table 1. It can be seen that the found refractive index values and the packing densities of S2 and S4 films are in good agreement with the refractive indices and the packing densities of S1 and S3 films, respectively. The slight differences in geometrical thicknesses can be attributed to different positions of S1, S3 and S2, S4 samples during the deposition process. The refractive indices and extinction coefficients of S2 and S4 films, found from *ex situ* data, are compared in Fig. 4. It can be seen that the refractive index of the S4 film is essentially higher than the refractive index of the S2 film produced at the relatively low substrate temperature. These observations are consistent with the results from [9,13]. The extinction coefficient of the S4 film is lower than the extinction coefficient of the S2 film. The densities of the films deposited at 300° (films S3 and S4) are higher than the densities of the TiO_2 films produced at 120° (films S1 and S2). These facts can be useful in the course of further study of potential applications of evaporated TiO_2 films.

4. Influence of Thermal Annealing on the Properties of TiO_2 Thin Films

In Figs. 5 and 6, we compare the spectral characteristics of samples S2 and S4 before and after annealing. It can be seen that the transmittances of both samples decreased after annealing and the decrease is greater in the case when the sample was deposited at a lower substrate temperature. The reflectances of the samples after annealing exhibit oscillations of larger amplitudes than the reflectances of these samples before annealing. This effect is more pronounced in the case of sample S2. It can be seen from Figs. 5 and 6 that the spectral curves corresponding to the samples after annealing are shifted to longer wavelengths with respect to the spectral curves before annealing. Based on this qualitative analysis of the measured spectral characteristics, we expected that the refractive indices and the extinction coefficients of S2 and S4 films would increase after annealing.

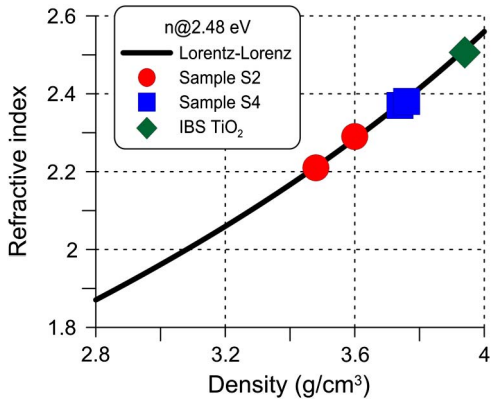

Fig. 3. Refractive indices of e-beam evaporated TiO_2 films at 500 nm before and after annealing (see Tables 1 and 2). The refractive index of IBS TiO_2 film is presented for comparison. Solid curve represents Lorentz–Lorenz dependence Eq. (4).

In Fig. 7 we present the determined refractive indices and extinction coefficients of S2 and S4 films before and after annealing. As expected, the refractive indices and the extinction coefficients of both films increased after annealing. This increase is quite distinctive in case of sample S2, which was deposited at a relatively low substrate temperature. These results are consistent with the ones obtained in [10].

The main parameters of S2 and S4 films are collected in Table 2. One can see that the geometrical thicknesses of layer S2 after annealing have decreased by about 2.5%. That can be attributed to expulsion of water from the sample and subsequent changes of the film stoichiometry. For the same reason, the density and the packing density of film S2 increased after annealing. In the case of the S4 sample, the geometrical thickness, packing density, and density changed insignificantly, by 0.5%–1%, which is comparable with the characterization accuracy.

We estimated the bandgaps of the films with the help of Tauc plots [31–33]. In high-absorption spectral range, the absorption coefficient α is related to the photon energy E in the following way [32,34,35]:

$$\alpha(E) = \frac{B(E - E_g)^m}{E}, \tag{5}$$

where B is a constant and m is a number characterizing the absorption process. This number takes the

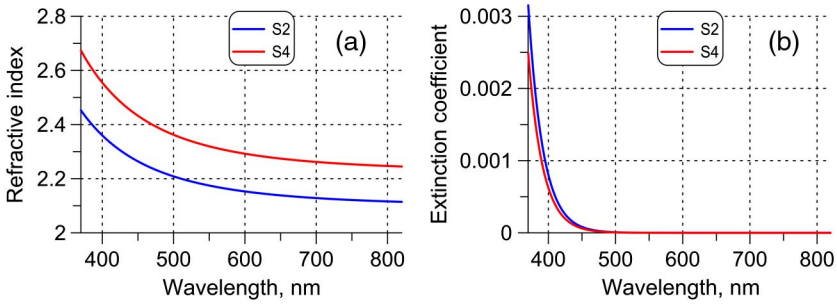

Fig. 4. (a) Refractive indices and (b) extinction coefficients of TiO_2 films deposited at different substrate temperatures.

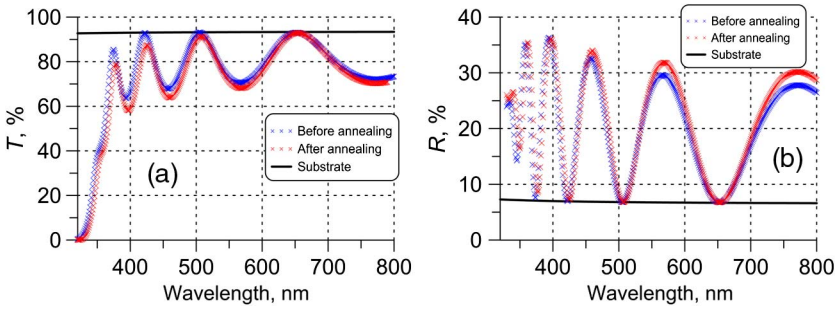

Fig. 5. (a) Transmittance and (b) reflectance spectra taken for sample S2 before and after annealing.

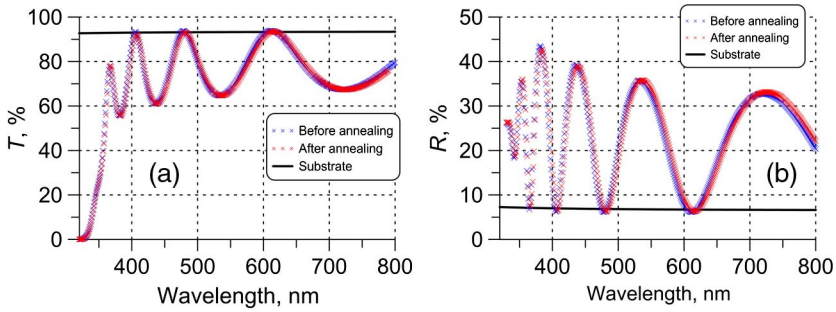

Fig. 6. (a) Transmittance and (b) reflectance spectra taken for sample S4 before and after annealing.

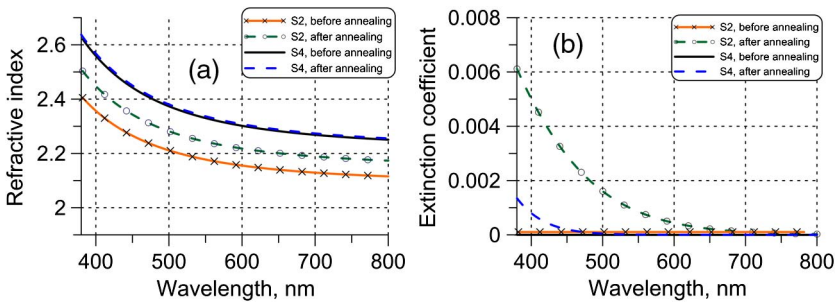

Fig. 7. (a) Refractive indices and (b) extinction coefficients of TiO_2 films before and after annealing.

Table 2. Parameters of TiO_2 Films before and after Annealing

	n at 500 nm		Thickness, nm		Density, g/cm^3		Packing Density, %	
Sample	Before	After	Before	After	Before	After	Before	After
S2	2.21	2.29	456.5	445.9	3.48	3.6	74.7	81.7
S4	2.37	2.38	398.6	400.9	3.7	3.75	88.1	89.0

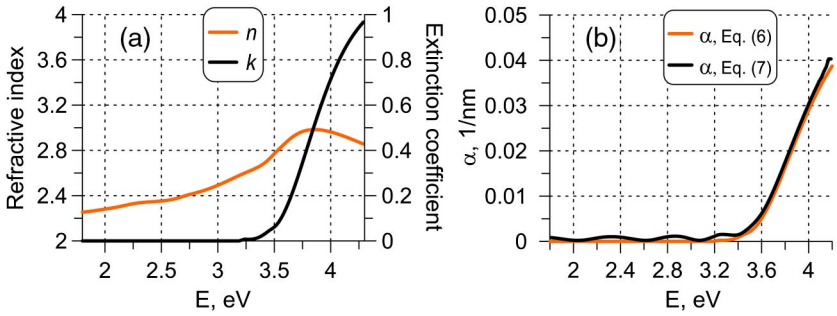

Fig. 8. (a) Model optical constants and (b) absorption coefficient of model sample calculated by Eqs. (6) and (7).

values 1/2 or 2 for direct and indirect transitions, respectively. If $m = 1/2$ or $m = 2$, then $(\alpha E)^2$ and $(\alpha E)^{1/2}$ have linear dependences on E. Thus, by plotting $(\alpha E)^2$ and $(\alpha E)^{1/2}$ versus E, fitting them by linear dependencies and extrapolating this linear fit to zero, one obtains direct and indirect bandgap energies, respectively.

The absorption coefficient

$$\alpha = \frac{4\pi}{\lambda} k(\lambda), \qquad E = \frac{1240}{\lambda}, \tag{6}$$

is expressed through extinction coefficient $k(\lambda)$. This coefficient is determined using a characterization process based on a thin film model. However, the characterization process in the short-wavelength spectral range requires the application of accurate models taking into account surface roughness. In addition to this, errors in T/R data affect the results. Hence, the dependence $k(\lambda)$, described by the exponential or the oscillator model and obtained from simultaneous fit of T/R data, might be considered as an estimation of extinction coefficient only. Another way to estimate absorption coefficient is to neglect the interference effects and scattering within the films and approximate α on the basis of Beer's law.

To estimate the bandgaps on the basis of experimental transmittance data, first we estimated absorption coefficient on the basis of Beer's law. According to this law, the absorption coefficient may be approximated as [5,6,32,36]

$$\alpha \approx -\frac{1}{d} \ln(T). \tag{7}$$

To estimate the accuracy of the approximation in Eq. (7), we excluded the influence of measurement errors and used model data. Let us consider a model TiO_2 film of 400 nm thickness on a transparent substrate of 1 mm thickness. The refractive index $n(\lambda)$ and the extinction coefficient $k(\lambda)$ of this film in the spectral range from 1.8 to 4.3 eV are shown in Fig. 8(a). In Fig. 8(b), we compare the absorption coefficients calculated using Eqs. (6) and (7). It is evident that they are quite close to each other. The indirect bandgap values were found to be 3.33 and 3.29 eV, and direct bandgap values were found to be 3.78 and 3.81 eV. The deviations between E_g values calculated using Eqs. (6) and (7) do not exceed 0.05 eV. This value can be considered as an accuracy of bandgap determination in this study. The indirect bandgap is between 3.3 and 3.4 eV, and the direct bandgap is between 3.7 and 3.8 eV. The difference between direct and indirect E_g values is 0.3–0.4 eV, which is also in agreement with the results of other authors (see, for example [6,12,34]).

In this study we estimated both direct and indirect bandgaps. The E_g values found for sample S2 are 3.75–3.8 eV (direct) and 3.4–3.5 eV (indirect), and the E_g values found for sample S4 are 3.45–3.5 eV (indirect) and 3.7–3.75 eV (direct). In Fig. 9, the Tauc plots for direct and indirect bandgaps and the corresponding linear fits for the case of S2 sample after annealing are presented. According to [37], in amorphous TiO_2 films one should expect the indirect type of absorption coefficient behavior rather than the direct type. Thus, bandgap values calculated using Eq. (5) with $m = 2$ should be considered as more reliable estimations. In our study we were interested

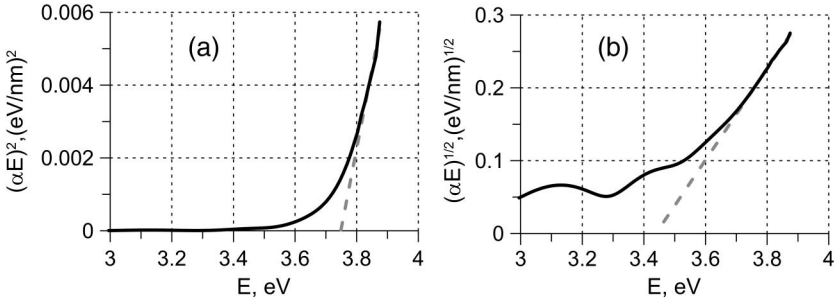

Fig. 9. Solid curves: (a) Tauc plots for the estimation of direct and (b) indirect band gaps; dashed lines: corresponding linear fits. The data are related to S2 sample after annealing.

not only in the numerical values of the bandgaps, but also in the relative shift of the bandgap values after annealing of the samples. We found that for both samples, S2 and S4, the bandgap values decreased after annealing. The increase of the refractive indices and the respective decrease of the bandgap values are consistent with quantum mechanical calculations presented in [20].

The E_g values, estimated in the present study are in agreement with the results of other authors. In [12], the values of direct bandgap of TiO_2 films deposited by e-beam evaporation at 300°C are estimated as 3.81–3.92 eV. In [6], indirect and direct bandgap values are in the ranges 3.39–3.42 eV and 3.67–3.72 eV. In [8], the indirect and direct E_g values are 3.39–3.42 eV and 3.68–3.70 eV, respectively. In [34], the values 3.75 and 3.4 eV are presented for direct and indirect bandgaps, respectively. It should be noted also that the differences between direct and indirect E_g values obtained in the present study are about 0.3–0.4 eV, which is in agreement with the results from the literature (see, for example [6,8,12,34]). The estimation of the bandgaps shows that from the point of view of laser applications, the annealing of multilayer coatings containing TiO_2 layers does not benefit their optical resistance for ultrashort pulses.

5. Conclusions

The reliable characterization of e-beam evaporated TiO_2 films provides a basis for careful studying of LIDT in multilayer coatings containing TiO_2 layers. Also, predicting *in situ* refractive indices of TiO_2 films and the vacuum shift allows for more accurate monitoring of multilayer coatings with TiO_2 layers. Annealing of the films does not lead to an increase but to a decrease of the bandgap, which is not beneficial for obtaining high LIDT of optical coatings containing TiO_2 layers in sub-10-ps pulse regime. At the same time, the refractive index and packing density of TiO_2 films are increased, that may be useful for other applications, including operation with pulses having nanosecond range durations.

This work was supported by the DFG Cluster of Excellence, "Munich Centre for Advanced Photonics," (http://www.munich-photonics.de).

References

1. H. K. Pulker, *Coatings on Glass* (Elsevier, 1999).
2. H. A. Macleod, *Thin-film Optical Filters*, 4th ed. (Taylor & Francis, 2010).
3. D. Mergel, D. Buschendorf, S. Eggert, R. Grammes, and B. Samset, "Density and refractive index of TiO_2 films prepared by reactive evaporation," Thin Solid Films **371**, 218–224 (2000).
4. M. Vergöhl, O. Werner, and S. Bruns, "New developments in magnetron sputter processes for precision optics," Proc. SPIE **7101**, 71010B (2008).
5. B. Zhao, J. Zhou, and L. Rong, "Microstructure and optical properties of TiO_2 thin films deposited at different oxygen flow rates," Trans. Nonferrous Met. Soc. China **20**, 1429–1433 (2010).
6. M. M. Hasan, A. S. M. A. Haseeb, R. Saidur, H. H. Masjuki, and M. Hamdi, "Influence of substrate and annealing temperatures on optical properties of RF-sputtered TiO_2 thin films," Opt. Mater. **32**, 690–695 (2010).
7. D. Yoo, I. Kim, S. Kim, C. H. Hahn, C. Lee, and S. Cho, "Effects of annealing temperature and method on structural and optical properties of TiO_2 films prepared by RF magnetron sputtering at room temperature," Appl. Surf. Sci. **253**, 3888–3892 (2007).
8. V. Mikhelashvili and G. Eisenstein, "Optical and electrical characterization of the electron beam gun evaporated TiO_2 film," Microelectron. Reliab. **41**, 1057–1061 (2001).
9. H. K. Pulker, G. Paesold, and E. Ritter, "Refractive indices of TiO_2 films produced by reactive evaporation of various titanium-oxygen phases," Appl. Opt. **15**, 2986–2991 (1976).
10. S.-H. Woo and C. K. Hwangbo, "Effects of annealing on the optical, structural, and chemical properties of TiO_2 and MgF_2 thin films prepared by plasma ion-assisted deposition," Appl. Opt. **45**, 1447–1455 (2006).
11. C.-C. Lee, H.-C. Chen, and C.-C. Jaing, "Investigation of thermal annealing of optical properties and residual stress of ion-beam-assisted TiO_2 thin films with different substrate temperatures," Appl. Opt. **45**, 3091–3096 (2006).
12. C. Yang, H. Fan, Y. Xi, J. Chen, and Z. Li, "Effects of depositing temperatures on structure and optical properties of TiO_2 film deposited by ion beam assisted electron beam evaporation," Appl. Surf. Sci. **254**, 2685–2689 (2008).
13. S. Schiller, G. Beister, W. Sieber, G. Schirmer, and E. Hacker, "Influence of deposition parameters on the optical and structural properties of TiO_2 films produced by reactive d.c. plasmatron sputtering," Thin Solid Films **83**, 239–245 (1981).
14. N. Ghrairi and M. Bouaicha, "Structural, morphological, and optical properties of TiO_2 thin films synthesized by the electrophoretic deposition technique," Nanoscale Res. Lett. **7**, 357–364 (2012).
15. R. Capan, N. B. Chaure, A. K. Hassan, and A. K. Ray, "Optical dispersion in spun nanocrystalline titania thin films," Semicond. Sci. Technol. **19**, 198–202 (2004).
16. K. Bange, C. R. Ottermann, O. Anderson, U. Jeschkowski, M. Laube, and R. Feile, "Investigations of TiO_2 films deposited by different techniques," Thin Solid Films **197**, 279–285 (1991).
17. H.-C. Chen, K.-S. Lee, and C.-C. Lee, "Annealing dependence of residual stress and optical properties of TiO_2 thin film deposited by different deposition methods," Appl. Opt. **47**, C284–C287 (2008).
18. A. V. Tikhonravov, M. K. Trubetskov, T. V. Amotchkina, G. DeBell, V. Pervak, A. K. Sytchkova, M. L. Grilli, and D. Ristau, "Optical parameters of oxide films typically used in optical coating production," Appl. Opt. **50**, C75–C85 (2011).
19. D. Reyes-Coronado, G. Rodríguez-Gattorno, M. E. Espinosa-Pesqueira, C. Cab, R. de Coss, and G. Oskam, "Phase-pure TiO_2 nanoparticles: anatase, brookite, and rutile," Nanotechnology **19**, 145605 (2008).
20. T. Amotchkina, M. Turowski, H. Ehlers, M. Jupé, and D. Ristau, "Bandgap and refractive index of TiO_2 films of different densities," in *OSA Technical Digest* (OSA, 2013), paper WA.4.
21. M. Landmann, T. Köhler, S. Köppen, E. Rauls, T. Frauenheim, and W. G. Schmidt, "Fingerprints of order and disorder in the electronic and optical properties of crystalline and amorphous TiO_2," Phys. Rev. B **86**, 064201 (2012).
22. H. G. Tompkins and E. A. Irene, *Handbook of Ellipsometry* (Springer, 2005).
23. M. Mero, J. Liu, W. Rudolph, D. Ristau, and K. Starke, "Scaling laws of femtosecond laser pulse induced breakdown in oxide films," Phys. Rev. B **71**, 115109 (2005).
24. B. Mangote, L. Gallais, M. Commandré, M. Mende, L. Jensen, H. Ehlers, M. Jupé, D. Ristau, A. Melninkaitis, J. Mirauskas, V. Sirutkaitis, S. Kičas, T. Tolenis, and R. Drazdys, "Femtosecond laser damage resistance of oxide and mixture oxide optical coatings," Opt. Lett. **37**, 1478–1480 (2012).
25. I. B. Angelov, A. von Conta, S. A. Trushin, Z. Major, S. Karsch, F. Krausz, and V. Pervak, "Investigation of the laser-induced

damage of dispersive coatings," Proc. SPIE **8190**, 81900B (2011).
26. B. Stuart, M. Feit, S. Herman, A. Rubenchik, B. Shore, and M. Perry, "Nanosecond-to-femtosecond laser-induced breakdown in dielectrics," Phys. Rev. B **53**, 1749–1761 (1996).
27. D. Ristau, H. Ehlers, T. Gross, and M. Lappschies, "Optical broadband monitoring of conventional and ion processes," Appl. Opt. **45**, 1495–1501 (2006).
28. D. Poelman and P. F. Smet, "Methods for the determination of the optical constants of thin films from single transmission measurements: a critical review," J. Appl. Phys. **36**, 1850–1857 (2003).
29. A. Tikhonravov, M. Trubetskov, and G. DeBell, "On the accuracy of optical thin film parameter determination based on spectrophotometric data," Proc. SPIE **5188**, 190–199 (2003).
30. D. A. G. Bruggeman, "Berechnung verschiedener physikalischer Konstanten von heterogenen Substanzen. I. Dielektrizitätskonstanten und Leitfähigkeiten der Mischkörper aus isotropen Substanzen," Ann. Phys. **416**, 636–664 (1935).
31. J. Tauc, R. Grigorovici, and A. Vancu, "Optical properties and electronic structure of amorphous germanium," Phys. Status Solidi B **15**, 627–637 (1966).
32. L.-J. Meng and M. P. dos Santos, "Investigations of titanium oxide films deposited by d.c. reactive magnetron sputtering in different sputtering pressures," Thin Solid Films **226**, 22–29 (1993).
33. I. B. Lucy, J. Beynon, and D. N. Waters, "Optical properties of co-evaporated Cu-GeO_2 thin cermet films," J. Mater. Sci. Lett. **15**, 515–518 (1996).
34. S. Valencia, J. M. Marín, and G. Restrepo, "Study of the bandgap of synthesized titanium dioxide nanoparticules using the sol-gel method and a hydrothermal treatment," Open Mater. Sci. J. **4**, 9–14 (2010).
35. M. Sreemany and S. Sen, "A simple spectrophotometric method for determination of the optical constants and band gap energy of multiple layer TiO_2 thin films," Mater. Chem. Phys. **83**, 169–177 (2004).
36. J. Aarik, A. Aidla, A.-A. Kiisler, T. Uustare, and V. Sammelselg, "Effect of crystal structure on optical properties of TiO_2 films grown by atomic layer deposition," Thin Solid Films **305**, 270–273 (1997).
37. O. Stenzel, *The Physics of Thin Film Optical Spectra: An Introduction*, Vol. **44** of Springer Series in Surface Sciences (Springer, 2005).